

28. V. Mariscal *et al.*, *Protist* **157**, 421 (2006).
29. D. B. Knaff, in *Oxygenic Photosynthesis: The Light Reactions*, D. R. Ort, C. F. Yocum, Eds. (Kluwer Academic, Dordrecht, Netherlands, 1996), vol. 4, pp. 333–361.
30. J. E. Backhausen, C. Kitzmann, P. Horton, R. Scheibe, *Photosynth. Res.* **64**, 1 (2000).
31. R. J. Norby, M. F. Cotrufo, P. Ineson, E. G. O'Neill, J. G. Canadell, *Oecologia* **127**, 153 (2001).
32. B. A. Hungate, J. S. Duker, M. R. Shaw, Y. Q. Luo, C. B. Field, *Science* **302**, 1512 (2003).
33. S. von Caemmerer, *Biochemical Models of Leaf Photosynthesis* (CSIRO Publishing, Collingwood, Australia, 2000).
34. T. D. Sharkey, C. J. Bernacchi, G. D. Farquhar, E. L. Singaas, *Plant Cell Environ.* **30**, 1035 (2007).
35. We thank C. van Kessel, L. Jackson, and E. Carlisle for their review of the manuscript. This research was supported by NSF grants IBN-03-43127 and IOS-08-18435, by the National Research Initiative Competitive grant number 2008-35100-04459 from the U.S. Department of Agriculture National Institute of

Food and Agriculture, and by a postdoctoral fellowship from Agencia Regional de Ciencia y Tecnología, Region de Murcia, Spain to J.S.R.A. A.J.B. is a paid consultant to the Monsanto Corporation.

#### Supporting Online Material

www.sciencemag.org/cgi/content/full/328/5980/899/DC1  
Materials and Methods  
References

28 December 2009; accepted 24 March 2010  
10.1126/science.1186440

# Resource Management Cycles and the Sustainability of Harvested Wildlife Populations

John M. Fryxell,<sup>1\*</sup> Craig Packer,<sup>2</sup> Kevin McCann,<sup>1</sup> Erling J. Solberg,<sup>3</sup> Bernt-Erik Sæther<sup>4</sup>

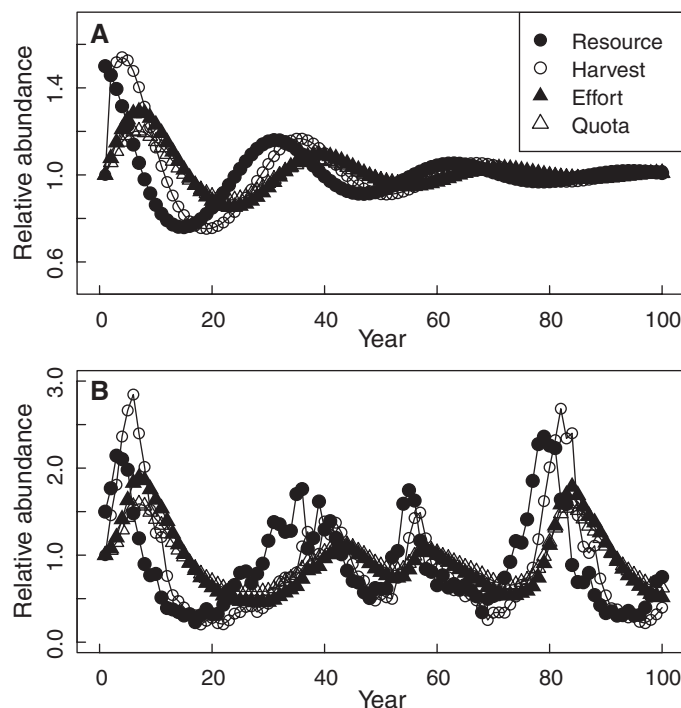
Constant harvest policies for fish and wildlife populations can lead to population collapse in the face of stochastic variation in population growth rates. Here, we show that weak compensatory response by resource users or managers to changing levels of resource abundance can readily induce harvest cycles that accentuate the risk of catastrophic population collapse. Dynamic system models incorporating this mix of feedback predict that cycles or quasi-cycles with decadal periodicity should commonly occur in harvested wildlife populations, with effort and quotas lagging far behind resources, whereas harvests should exhibit lags of intermediate length. Empirical data gathered from three hunted populations of white-tailed deer and moose were consistent with these predictions of both underlying behavioral causes and dynamical consequences.

One of the most central problems in ecology is what causes some harvested populations to collapse, whereas others are able to withstand exploitation (*I–4*)? Population collapses in many fisheries have encouraged substantial theoretical work on the challenging problem of optimal harvesting policy in response to demographic and environmental stochasticity (*I–8*). This has led to several sophisticated optimal harvest models supporting constant harvest mortality rates, threshold harvesting policies, or no-take reserves. Although these policies are sometimes feasible, in reality many management agencies have limited ability to control the number of resource users or harvest effort. This is particularly true of recreational harvesting, because of the open-access philosophy underlying sport fisheries and wildlife hunting. Even when harvest levels are directly set by regional managers, such control is often in the form of ad hoc quotas that vary from year to year. Modern harvesting theory is based on coupling harvest with dynamic variation in resource abundance. Here we show that weak compensatory response by harvesters or resource managers can itself gen-

erate cyclic variation in resources, exacerbating the risk of collapse. Weak harvest regulation contributes to the problem rather than providing an acceptable management solution to resource fluctuation.

To consider this issue, we developed a dynamical system model in discrete time (*9*), based on simple intuitive assumptions about human

**Fig. 1.** Predicted time series for the proposed dynamic harvest-effort-quota system, for a locally stable set of parameters ( $a = 0.3$ ,  $K = 4$ ,  $q = 0.0001$ ,  $c = -0.1$ ,  $w = 0.2$ ,  $u = 0.00002$ ,  $f = -0.05$ ,  $i = 0.15$ ,  $j = 0.1$ ) (*9*) (A) without any environmental stochasticity and (B) with the standard deviation in environmental stochasticity ( $\epsilon = 0.20$ ). To simplify plotting on a single set of axes, variables were normalized by dividing yearly values by equilibrium values.



<sup>1</sup>Department of Integrative Biology, University of Guelph, 50 Stone Road East, Guelph, Ontario N1G 2W1, Canada. <sup>2</sup>Department of Ecology, Evolution, and Behavior, University of Minnesota, 1987 Upper Buford Circle, St. Paul, MN 55108, USA. <sup>3</sup>Norwegian Institute for Nature Research, Tungasletta 2, N-7485 Trondheim, Norway. <sup>4</sup>Centre for Conservation Biology, Department of Biology, Realfagbygget, NTNU, 7491 Trondheim, Norway.

\*To whom correspondence should be addressed. E-mail: jfryxell@uoguelph.ca

nual modification of quotas. Our model also assumes that managers are reluctant to exceed quota levels experienced in the past, leading to a negative feedback on rates of quota change (9).

These compensatory responses can be readily incorporated into a modified version of the Rosenzweig-MacArthur model of consumer-resource interactions (11, 12). We consider a discrete time formulation to be more realistic than a continuous formulation for several reasons: (i) most fish and wildlife species of interest have a single birth-pulse breeding season each year, (ii) harvesting is typically confined to a short season each year, and (iii) license sales and quota levels are usually set in advance of the harvest season. We accordingly structured our discrete time model by assuming that harvesting is followed by density-dependent recruitment according to the Ricker logistic formulation, with negative feedbacks on the exponential rate of population growth dictated by post-harvest resource abundance (9). For subsequent analyses of the deterministic form of the discrete time model, we re-scaled state variables to make them dimensionless. Local stability analysis (9) was used to compare the range of stable versus unstable parameter combinations, to determine whether damped oscillations characterize the response to local perturbations from equilibria and to estimate the period length of such damped oscillations (13–16).

In the absence of environmental stochasticity, our model predicts that equilibria are locally stable for a restricted set of parameter combinations, whereas stable limit cycles are the norm for other parameter combinations, a pattern often seen in ecological models (12–16). Deterministic instability is particularly likely when resource carrying capacity is high, the maximum rates of increase in effort or quotas are particularly high, or the rate of decline in effort or quotas at low resource abundance is particularly low (fig. S1). Even in stable systems, however, our model predicts that the approach to stability after perturbation will be extremely slow, characterized by damped oscillations over time (Fig. 1A). The return time for such damped cycles depends on intrinsic growth rates, but for many large-bodied species, including most mammals, birds, and sport fish, it may take decades for perturbed populations to recover their former abundance (fig. S2).

In the real world, populations are invariably subject to substantial levels of environmental and/or demographic stochasticity (17, 18). Damped oscillations in the deterministic system coupled with stochastic variation in population growth rates leads to quasi-cyclic fluctuation (15, 16) (Fig. 1B), with similar periodicity as that seen in simpler perturbed systems (Fig. 1A). In other words, dynamic variation in harvest effort and/or quotas, coupled with environmental or demographic stochasticity, should often lead to wildlife population cycles regardless of other ecological interactions.

Instability in our model traces from asynchrony in the dynamic responses of either harvesters or their regulating agencies to changes in resource

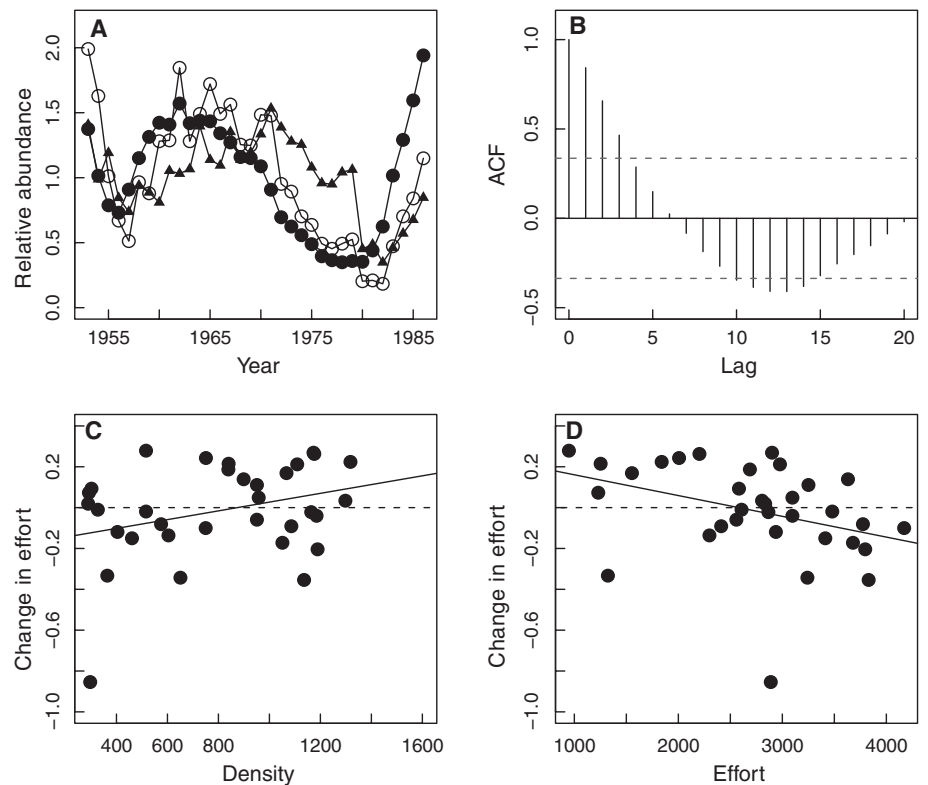


**Fig. 2.** Harvest data are illustrated for white-tailed deer from the Canonto District of Ontario, Canada. (A) Annual estimates of resource abundance (solid circles), harvest (open circles), and effort (solid triangles). To simplify plotting on a single set of axes, variables were normalized by dividing yearly values by the mean for the entire time series. Autocorrelation functions for resource abundance are shown in (B). All sample autocorrelation function values that exceed the horizontal bars are statistically significant ( $P < 0.05$ ). The bottom two plots show rates of change in hunting effort ( $z$ ) in relation to resource density ( $x$ ) (C) and current effort ( $y$ ) (D) ( $z = 0.0706 + 0.000305x - 0.000104y$ ,  $F_{2,30} = 5.51$ ,  $P = 0.009$ ,  $R^2 = 0.271$ ).

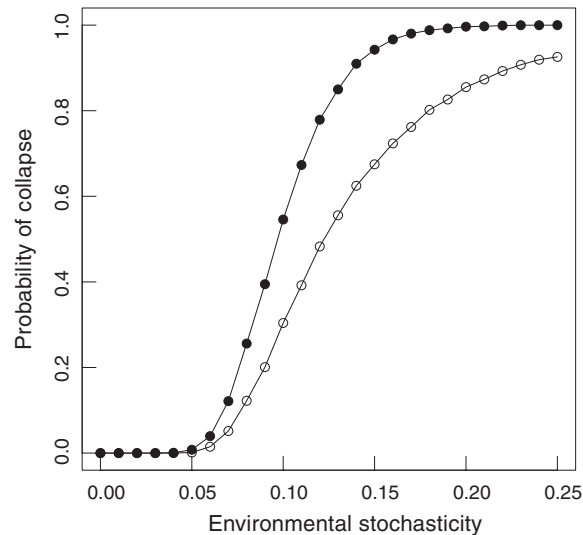
levels. Social adjustments in effort or regulatory adjustments in quotas occur at discrete, annual intervals because of short harvest season lengths. As a consequence, even locally stable systems would require a long time to equilibrate. In a realistically noisy world, such slow equilibration would translate into quasi-cycles of extended length, typically on the order of decades. The propensity for quasi-cyclic fluctuations is more pronounced for species with low intrinsic growth rates and modest levels of environmental stochasticity, such as large mammals, than it is for species with faster life histories or those subject to high variation in environmental conditions.

Our model suggests that harvested species are regulated by either harvester behavior or management policy, but not both. The structure of the model is such that either effort or quotas fully determine system equilibria, depending on which regulatory process supports the higher level of resources at equilibrium. Because both processes respond to changes in resource abundance, however, time dynamics of effort and quotas in unstable systems should become synchronized (Fig. 1B). Our model makes a number of testable predictions: (i) rates of change in effort and quotas should be positively associated with resource levels,

but negatively related to current levels of effort or quotas; (ii) harvested populations should often fluctuate with return times on the order of decades; and (iii) both effort and quotas should fluctuate in unison, but each should be far out of phase with resources, whereas harvest should have a lag of intermediate length.

As a proof of concept, we evaluated our model using three different populations of hunted ungulates (Canadian white-tailed deer and Norwegian moose) that had at least 20 years of continuous time series data available on population density, harvest, effort, and quota. Moose data for the Troms and Vest Agder Districts in Norway were provided by the National Moose-Monitoring Program (19). For the purposes of this paper, population abundance was estimated using moose seen per hunter day. Data on harvest level and hunter effort came from hunter questionnaires with high response rates. Data for white-tailed deer came from the Canonto District of Ontario. Deer harvests during 1953–1987 were limited to a 1- to 2-week period during the autumn. Access to the site was limited to two roads, both of which were closely monitored by wildlife personnel, who interviewed every hunter leaving the area to estimate hunt-

**Fig. 3.** Predicted probability of population collapse (to 10% of the equilibrium density) in a model system with constant effort (open circles) compared to one with weak compensatory changes in effort (solid circles), based on 5000 Monte Carlo replicates for each level of environmental stochasticity. Constant effort and quota levels were set at equilibria for the dynamic system. Simulations were based on the same locally stable set of parameters shown in Fig. 1 ( $a = 0.3$ ,  $K = 4$ ,  $q = 0.0001$ ,  $c = -0.1$ ,  $w = 0.2$ ,  $u = 0.00002$ ,  $f = -0.05$ ,  $i = 0.15$ ,  $j = 0.1$ ) with the standard deviation in environmental stochasticity  $\varepsilon$  ranging between 0.00 and 0.25.



ing effort (days) and harvest. Deer population density in the 230-km<sup>2</sup> study area was estimated with virtual population analysis (20). For all study populations, exponential rates of increase in effort and quotas were estimated by  $y_t = \ln(x_{t+1}/x_t)$ , where  $y$  is the exponential rate of change,  $x$  is the response variable (either effort or quota), and  $t$  is time, measured in years. Linear regression was used to test whether rates of increase in effort and quotas were significantly related to resource abundance and current levels of either effort or quota. Standard time series analyses (autocorrelation and cross-correlation functions in the statistical software R, version 2.4) were applied to each data set to evaluate statistical support for recurrent versus damped oscillations and lag length for harvest, effort, and quotas relative to resource abundance (15). Although complete understanding of the population dynamics of long-lived species is enhanced by age-specific data on demographic rates (21), simpler nonstructured models, such as the Ricker equation used here, can often be used to capture the most salient dynamical features (15, 22). Simpler models have the added benefit of allowing the full range of analytical tools needed to evaluate the stability of complex dynamic systems.

All of the populations exhibited diagnostic patterns that were remarkably consistent with our model (Fig. 2 and figs. S3 and S4). Population abundance varied considerably over time, with the smallest range of variation recorded in moose in the Troms District (twofold) and the highest variability recorded in white-tailed deer (fivefold). In each population, autocorrelation functions provided evidence of phase-forgetting (damped) oscillations in resource abundance, with period lengths of 8, 24, and 30 years. Cross-correlation functions indicated a pronounced lag (2 to 6 years) between fluctuations in resource abundance and effort, a modest lag between harvest and effort, and little lag between quotas and effort (fig. S5). Changes in effort were pos-

itively related to resource abundance but negatively related to current levels of effort. Rates of change in quotas were also positively related to resource abundance but negatively related to quota level (fig. S6). All of these time series characteristics were predicted by the model.

Alternatively, changes in harvesting pressure can induce generational cycles in long-lived species by perturbations of the stable age distribution (21–23). We tested this possibility by time series analysis of the proportion of deer and moose young through time. Although strong cohorts were identified in all three study populations, autocorrelation functions showed no evidence of cyclic fluctuation in age structure that could explain the observed oscillations in overall population abundance (figs. S7 and S8). Thus, although it is theoretically possible that temporal variation in age structure can interact with harvest dynamics and population abundance to amplify unstable dynamics, generation cycles do not explain the observed oscillations in the abundance of white-tailed deer and moose.

Wildlife harvesting of species such as moose, elk, deer, bears, bobcats, and cougars is often conducted in a manner consistent with our model. In many jurisdictions, virtually anyone is eligible to apply for a hunting permit. There are often regional quotas on harvest, however, facilitated via telephone hotlines. Although there can be special restrictions on the age, sex, or location of harvested animals, regulatory procedures for a given species often tend to be fairly consistent across different wildlife agencies.

As a result of the open-access philosophy typically underlying wildlife harvest management (that is, employing few restrictions on participation in hunting, instead changing quotas on an annual basis), large-scale fluctuations in abundance are to be expected. A scattering of published papers in the literature are consistent with the unstable scenario we have drawn (1, 24–27), suggesting that quasi-periodic fluctuations in resources, exploitation rate, and quotas may be

much more common than previously realized. If we are correct in asserting that asynchronous dynamics of harvested resources, effort, and quotas often occur, due to delayed human behavioral responses to changing conditions, then conservation and management agencies might well benefit from more frequent reassessment of quota levels in response to undesirable changes in population levels occurring over the course of the hunting season, or from the institution of more conservative, temporally stable policies. Future harvest policies should aim to minimize variation in resource mortality risk by maintaining constant effort, setting quotas proportionate to current resource abundance, or shifting to threshold or proportional threshold approaches. Reconciling these alternative management options with open-access policies will no doubt prove challenging.

Weak harvest regulation should be particularly worrisome in populations with high levels of demographic or environmental stochasticity or with pronounced Allee effects due to predation, disease transmission, or reduced probability of breeding (28–30). Our simulations suggest that the risk of population collapse could be dramatically higher in systems with dynamic effort and quota levels (Fig. 3), simply because of extreme population excursions caused by quasi-periodic dynamics resulting from even mild levels of environmental stochasticity. When resource abundance is regulated by dynamic management responses via quotas, unstable systems are often vulnerable to extinction, even in the absence of Allee effects or stochastic variation in growth rates. These findings suggest that it is unwise to neglect dynamic patterns of change in both harvest effort and quotas in assessing long-term strategies for sustainable resource use.

#### References and Notes

1. B. Worm *et al.*, *Science* **325**, 578 (2009).
2. C. N. K. Anderson *et al.*, *Nature* **452**, 835 (2008).
3. J. R. Beddington, R. M. May, *Science* **197**, 463 (1977).
4. C. W. Clark, *Mathematical Bioeconomics: The Optimal Management of Renewable Resources* (Wiley, New York, 1990).
5. R. Lande, B.-E. Saether, S. Engen, *Ecology* **78**, 1341 (1997).
6. M. Mangel, *Ecol. Lett.* **1**, 87 (1998).
7. A. Hastings, L. W. Botsford, *Science* **284**, 1537 (1999).
8. M. G. Neubert, *Ecol. Lett.* **6**, 843 (2003).
9. Detailed materials and methods are provided in the supporting material on Science Online.
10. M. Schaefer, *Inter-Am. Trop. Tuna Comm. Bull.* **1**, 27 (1954).
11. M. L. Rosenzweig, R. H. MacArthur, *Am. Nat.* **97**, 209 (1963).
12. M. L. Rosenzweig, *Science* **171**, 385 (1971).
13. A. Hastings, *Population Biology: Concepts and Models* (Springer, New York, 1997).
14. S. P. Otto, T. Day, *A Biologist's Guide to Mathematical Modelling* (Princeton Univ. Press, Princeton, NJ, 2007).
15. P. Turchin, *Complex Population Dynamics* (Princeton Univ. Press, Princeton, NJ, 2003).
16. R. M. Nisbet, W. S. C. Gurney, *Modelling Fluctuating Populations* (Wiley, Chichester, UK, 1982).
17. M. Boyce, C. Haridas, C. Lee, *Trends Ecol. Evol.* **21**, 141 (2006).
18. R. Lande, S. Engen, B.-E. Saether, *Stochastic Population Dynamics in Ecology and Conservation* (Oxford Univ. Press, Oxford, 2003).
19. E. J. Solberg, B.-E. Saether, O. Strand, A. Loison, *J. Anim. Ecol.* **68**, 186 (1999).

20. J. M. Fryxell, D. J. T. Hussell, A. B. Lambert, P. C. Smith, *J. Wildl. Manage.* **55**, 377 (1991).
21. A. Beckerman, T. G. Benton, E. Ranta, V. Kaitala, P. Lundberg, *Trends Ecol. Evol.* **17**, 263 (2002).
22. T. Coulson *et al.*, *Ecology* **89**, 1661 (2008).
23. T. Coulson, F. Guinness, J. Pemberton, T. Clutton-Brock, *Ecology* **85**, 411 (2004).
24. G. Bell, P. Handford, C. Dietz, *J. Fish. Res. Board Can.* **34**, 842 (1977).
25. A. A. Berryman, *Oikos* **62**, 106 (1991).
26. R. McGarvey, *Can. J. Fish. Aquat. Sci.* **51**, 900 (1994).
27. C. Packer *et al.*, *PLoS ONE* **4**, e5941 (2009).
28. F. Courchamp, T. Clutton-Brock, B. Grenfell, *Trends Ecol. Evol.* **14**, 405 (1999).
29. P. A. Stephens, W. J. Sutherland, *Trends Ecol. Evol.* **14**, 401 (1999).
30. B. A. Melbourne, A. Hastings, *Nature* **454**, 100 (2008).
31. This work was supported by Discovery Grants to J.M.F. and K.M. from the Natural Sciences and Engineering Research Council of Canada, and NSF Grants for Long-Term Research in Environmental Biology and Biocomplexity to C.P. The contributions by B.E.S. and E.J.S. were funded by the Directorate for Nature Management and the Norwegian Research Council (Changing Landscapes, Lanskap i Endring, and project

196304/V40). We thank A. Fryxell, T. Avgar, M. Anderson, T. Nudds, and two anonymous reviewers for helpful suggestions. Details of the dynamical stability analysis are available on request from the senior author.

### Supporting Online Material

www.sciencemag.org/cgi/content/full/328/5980/903/DC1  
Materials and Methods

Figs. S1 to S8  
Tables S1 to S5  
References

10 December 2009; accepted 24 March 2010  
10.1126/science.1185802

# Molecular Identity of Dendritic Voltage-Gated Sodium Channels

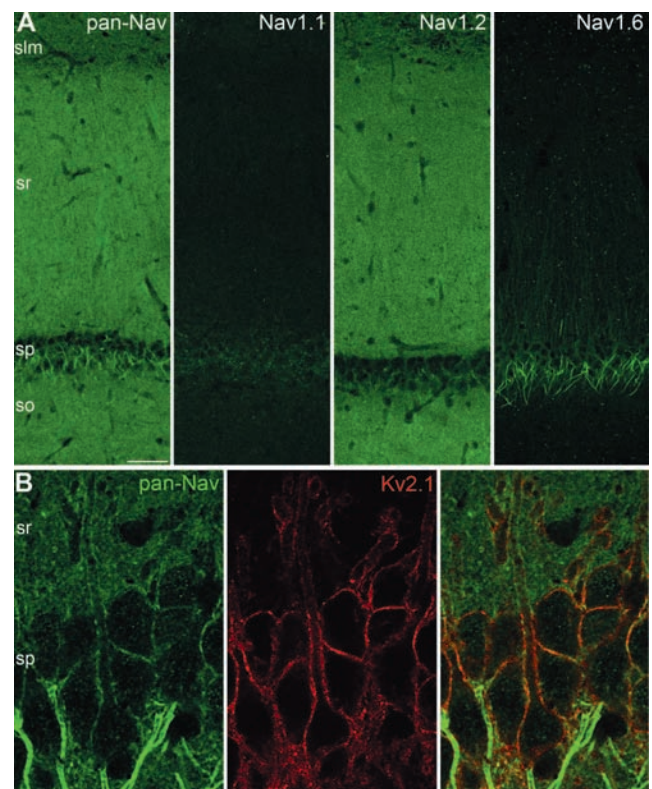
Andrea Lorincz\* and Zoltan Nusser\*

Active invasion of the dendritic tree by action potentials (APs) generated in the axon is essential for associative synaptic plasticity and neuronal ensemble formation. In cortical pyramidal cells (PCs), this AP back-propagation is supported by dendritic voltage-gated  $\text{Na}^+$  (Nav) channels, whose molecular identity is unknown. Using a highly sensitive electron microscopic immunogold technique, we revealed the presence of the Nav1.6 subunit in hippocampal CA1 PC proximal and distal dendrites. Here, the subunit density is lower by a factor of 35 to 80 than that found in axon initial segments. A gradual decrease in Nav1.6 density along the proximodistal axis of the dendritic tree was also detected without any labeling in dendritic spines. Our results reveal the characteristic subcellular distribution of the Nav1.6 subunit, identifying this molecule as a key substrate enabling dendritic excitability.

Associative synaptic plasticity in cortical pyramidal cells (PC) is the most widely accepted cellular model of learning. An essential prerequisite of the model is that input synapses, which are distributed over an enormously large dendritic tree, must be capable of sensing the precise timing of the output signal. The most likely mechanism for this is the active invasion of the dendritic tree by fast sodium action potentials (APs) initiated in the axon initial segment (AIS). Modification of back-propagating APs therefore holds tremendous potential for altering synaptic plasticity and forming of neuronal representations. Voltage-gated  $\text{Na}^+$  (Nav) currents have been detected in hippocampal and neocortical PC dendrites, where they not only support AP back-propagation but also underlie nonlinear synaptic integration and dendritic sodium spike generation [(1–6) and reviewed in (7–10)]. Patch-clamp experiments demonstrate that axonal and somatodendritic Nav currents differ in their activation and inactivation properties (11, 12), indicating either different Nav subunit compositions or distinct posttranslational modifications of identical subunits (12–14). However, the lack of subunit-specific drugs precludes the unequivocal identification of the subunit composition of the axosomatodendritic Nav channels using

functional approaches. Immunohistochemistry with subunit-specific antibodies offers an alternative experimental approach to address this issue. Nav1.1, Nav1.2, and Nav1.6 are the Nav subunits expressed in adult brains (15, 16). They have been

**Fig. 1.** Somatodendritic localization of voltage-gated sodium channels. (A) Immunofluorescence localization of the pan-Nav, Nav1.1, Nav1.2, and Nav1.6 subunits in the CA1 area. (B) Double immunofluorescence reaction shows weak pan-Nav immunolabeling along the Kv2.1 subunit immunoreactive somatodendritic plasma membrane of CA1 PCs. Note the much higher labeling intensity of the AISs. slm, stratum lacunosum-moleculare; sr, stratum radiatum; sp, stratum pyramidale; so, stratum oriens. Scale bars: (A), 50  $\mu\text{m}$ ; (B), 10  $\mu\text{m}$ .



Laboratory of Cellular Neurophysiology, Institute of Experimental Medicine, Hungarian Academy of Sciences, 1083 Budapest, Hungary.

\*To whom correspondence should be addressed. E-mail: nusser@koki.hu (Z.N.); lorincz@koki.hu (A.L.)



## Supporting Online Material for

### **Resource Management Cycles and the Sustainability of Harvested Wildlife Populations**

John M. Fryxell,\* Craig Packer, Kevin McCann, Erling J. Solberg, Bernt-Erik Sæther

\*To whom correspondence should be addressed. E-mail: [jfryxell@uoguelph.ca](mailto:jfryxell@uoguelph.ca)

Published 14 May 2010, *Science* **328**, 903 (2010)

DOI: 10.1126/science.1185802

**This PDF file includes:**

Materials and Methods  
Figs. S1 to S8  
Tables S1 to S5  
References

## Supporting online material

### Materials and methods

Random search theory (S1) predicts that harvest ( $H$ ) should be an exponential function of resource density ( $N$ ) and effort ( $E$ ), so long as the quota ( $Q$ ) is not exceeded. Assuming that density-dependent recruitment precedes harvest in any given year, typical of many harvested fish and wildlife populations, then harvest in year  $t$  is calculated as follows:

$$H_t = \min(N_t \cdot e^{a \cdot (1 - N_t / K) + \varepsilon_t} \cdot (1 - e^{-q \cdot E_t}), Q_t) \quad (1)$$

where  $a$  = maximum rate of increase of the resource,  $K$  = carrying capacity of the resource,  $q$  = the proportion of the resource population removed by one unit of effort.

Each year there is some degree of environmental stochasticity of magnitude  $\varepsilon_t$ , drawn from a normal distribution with standard deviation  $\sigma$  (S2). Resources, effort, and quotas in year  $t+1$  are calculated in the following manner:

$$N_{t+1} = \max(N_t \cdot e^{a \cdot (1 - N_t / K) - q \cdot E_t + \varepsilon_t}, N_t \cdot e^{a \cdot (1 - N_t / K) + \varepsilon_t} - Q_t) \quad (2)$$

$$E_{t+1} = E_t \cdot e^{c + w \cdot N_t - u \cdot E_t} \quad (3)$$

$$Q_{t+1} = Q_t \cdot e^{f + i \cdot N_t - j \cdot Q_t} \quad (4)$$

where  $c$  = constant for the exponential rate of change in effort,  $w$  = effect of one unit increase in resource density on the exponential rate of change in effort, and  $u$  = effect of one unit increase in effort on the exponential rate of change in effort. In similar fashion,  $f$  = constant for the exponential rate of increase in quotas,  $i$  = effect of one unit increase in resource density on the exponential rate of change in quotas, and  $j$  = effect of one unit increase in quotas on the exponential rate of change in quotas.

To simplify the local stability analysis, we re-scaled the dynamic effort and quota model (eq. 1-4), resulting in a new set of aggregate parameters: ( $b = wK$ ,  $d = uwK/q$ ,  $g = iK$ , and  $h = jK$ ) and a set of dimensionless variables ( $X = N/K$ ,  $Y = qE/wK$ ,  $W = H/K$ , and  $Z = Q/K$ ). The dimensionless model has the following structure (disregarding environmental stochasticity):

$$X_{t+1} = \max(X_t \cdot e^{a \cdot (1-X_t) - b \cdot Y_t}, X_t \cdot e^{a \cdot (1-X_t)} - Z_t) \quad (5)$$

$$Y_{t+1} = Y_t \cdot e^{c + b \cdot X_t - d \cdot Y_t} \quad (6)$$

$$Z_{t+1} = Z_t \cdot e^{f + g \cdot X_t - h \cdot Z_t} \quad (7)$$

The structure of these equations is such that either effort or quotas regulate resource density at equilibrium, but not both state variables. We first find the equilibrium resource density for each state variable in isolation. By identifying which of these potential equilibria occurs at the highest resource density, we can identify which process is regulating:

$$X_{eq1} = \frac{a \cdot d - b \cdot c}{b^2 + a \cdot d} \quad (8)$$

$$X_{eq2} = \text{root}(h \cdot X \cdot \exp(a \cdot (1 - X)) - 1) - g \cdot X - f \quad (9)$$

$$X_{eq} = \max(X_{eq1}, X_{eq2}) \quad (10)$$

Other equilibria are calculated as follows:

$$Y_{eq} = \frac{a + (1 - X_{eq})}{b} \quad (11)$$

$$Z_{eq} = \frac{f + g \cdot X_{eq}}{h} \quad (12)$$

$$W_{eq} = \min(X_{eq} \cdot \exp(a \cdot (1 - X_{eq}) \cdot (1 - \exp(-b \cdot Y_{eq}))), Z_{eq}) \quad (13)$$

For all models of this form, stability properties depend on the magnitude of the elements of the community interaction matrix ( $\alpha_{ij}$ ), evaluated at equilibria for the system ( $X_{eq}$  and either  $Y_{eq}$  or  $Z_{eq}$ )(S3-S7). For notational convenience we use the subscript 1 to refer to resources, 2 to refer to effort, and 3 to refer to quotas. Expressions for the community matrix coefficients are calculated in the following manner. If resources are regulated by effort, then community matrix coefficients are calculated as follows:

$$\alpha_{11} = (1 - a \cdot X_{eq}) \cdot e^{a \cdot (1 - X_{eq}) - b \cdot Y_{eq}} \quad (14)$$

$$\alpha_{12} = -b \cdot X_{eq} \cdot e^{a \cdot (1 - X_{eq}) - b \cdot Y_{eq}} \quad (15)$$

$$\alpha_{21} = b \cdot Y_{eq} \cdot e^{c + b \cdot X_{eq} - d \cdot Y_{eq}} \quad (16)$$

$$\alpha_{22} = (1 - d \cdot Y_{eq}) \cdot e^{c + b \cdot X_{eq} - d \cdot Y_{eq}} \quad (17)$$

If resources are regulated at equilibrium by quotas, then community matrix coefficients are calculated as follows:

$$\alpha_{11} = (1 - a \cdot X_{eq}) \cdot e^{\alpha \cdot (1 - X_{eq})} \quad (18)$$

$$\alpha_{13} = -1 \quad (19)$$

$$\alpha_{31} = g \cdot Z_{eq} \cdot e^{f + g \cdot X_{eq} - h \cdot Z_{eq}} \quad (20)$$

$$\alpha_{33} = (1 - h \cdot Z_{eq}) \cdot e^{f + g \cdot X_{eq} - h \cdot Z_{eq}} \quad (21)$$

The system will be locally stable, provided that the absolute values of the eigenvalues ( $\lambda$ ) of the community matrix are less than 1. These coefficients are also used to estimate whether equilibria represent stable foci, stable nodes, or saddle points and to estimate the period for damped oscillations. If resources are regulated at equilibrium by effort, then eigenvalues are calculated as follows (S4):

$$\lambda = (\frac{1}{2}) \cdot (\alpha_{11} + \alpha_{22} \pm \sqrt{(\alpha_{11} - \alpha_{22})^2 + 4 \cdot \alpha_{12} \cdot \alpha_{21}}) \quad (22)$$

If resources are regulated at equilibrium by quotas, then eigenvalues are calculated as follows (S4):

$$\lambda = (\frac{1}{2}) \cdot (\alpha_{11} + \alpha_{33} \pm \sqrt{(\alpha_{11} - \alpha_{33})^2 + 4 \cdot \alpha_{13} \cdot \alpha_{31}}) \quad (23)$$

For realistic parameter values, the eigenvalues always form complex conjugate pairs, with real ( $\varphi$ ) and imaginary ( $\psi$ ) parts. If resources are regulated by effort at equilibrium, then these parts are calculated in the following manner (S4):

$$\varphi = (\frac{1}{2}) \cdot (\alpha_{11} + \alpha_{22}) \quad (24)$$

$$\psi = (\frac{1}{2}) \cdot \sqrt{-(\alpha_{11} - \alpha_{22})^2 - 4 \cdot \alpha_{12} \cdot \alpha_{21}} \quad (25)$$

If resources are regulated by quotas at equilibrium, then the real and imaginary parts of the complex conjugate pairs are calculated in the following manner (S4):

$$\varphi = (\frac{1}{2}) \cdot (\alpha_{11} + \alpha_{33}) \quad (26)$$

$$\psi = (\frac{1}{2}) \cdot \sqrt{-(\alpha_{11} - \alpha_{33})^2 - 4 \cdot \alpha_{13} \cdot \alpha_{31}} \quad (27)$$

Equilibria are locally stable when

$$\sqrt{\varphi^2 + \psi^2} < 1 \quad (28)$$

The period of oscillations following perturbation scales in the following manner (S4):

$$\rho = \frac{2 \cdot \pi}{a \tan(\psi/\varphi)} \quad (29)$$

## Figures and legends

Fig. S1 – Locally stable (shaded) and unstable (unshaded) parameter combinations, based on eigenvalue analysis (4).

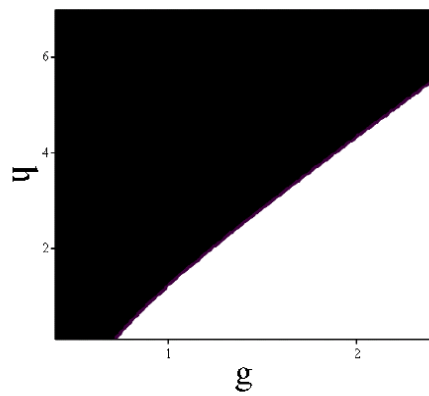
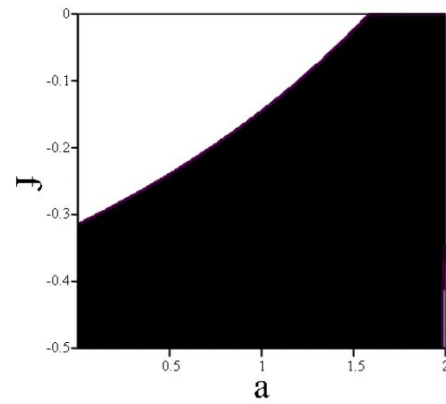
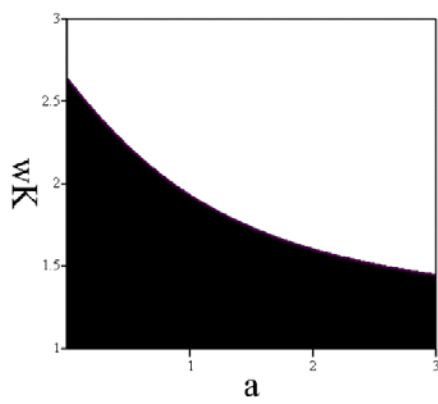


Fig. S2 - Predicted period (in years) of recurrent or damped oscillations for the proposed dynamic harvest-effort-quota model in relation to two key parameters: the maximum rate of change in effort ( $w \cdot K$ ) and the maximum rate of resource growth ( $a$ ).

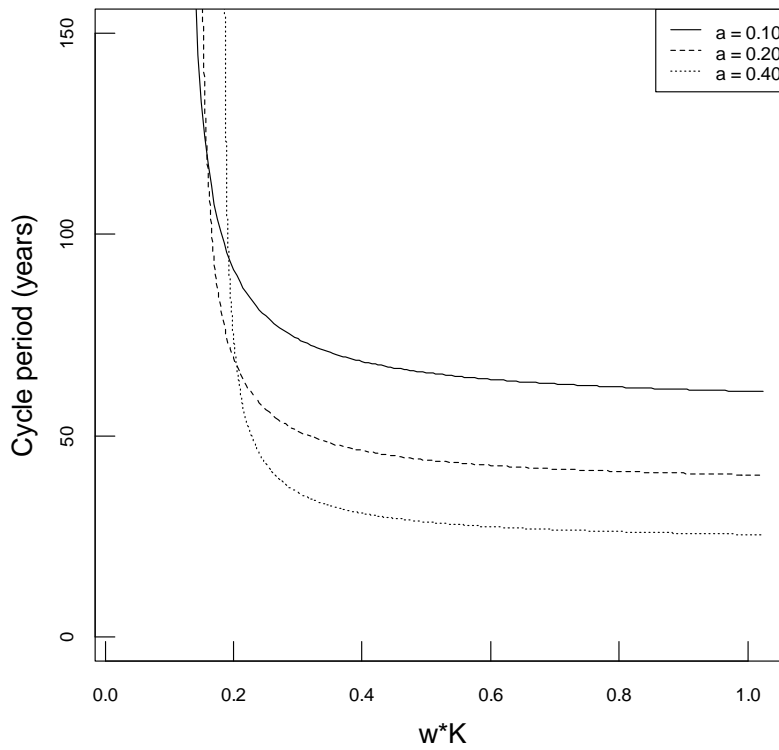


Fig. S3 – Harvest data for moose from the Vest Agder District (resource abundance (filled circles), harvest (open circles), and effort (filled triangles)). Variables were normalized by dividing yearly values by the mean for the entire time series. Auto-correlation functions for resource abundance are shown in the right-hand plot on the top row. All correlation coefficients that exceed the horizontal bars are statistically significant (Bartlett's Test,  $P < 0.05$ ). The bottom two plots show rates of change in hunting effort ( $z$ ) in relation to resource density ( $x$ ) and current effort ( $y$ ) (Vest Agder:  $z = -0.0925 + 0.181x - 0.00000976y$ ,  $F_{2,21} = 4.555$ ,  $P = 0.023$ ,  $R^2 = 0.303$ ; Troms:  $z = 0.0112 + 0.0618x - 0.0000237y$ ,  $F_{2,16} = 6.653$ ,  $P = 0.001$ ,  $R^2 = 0.454$ ).

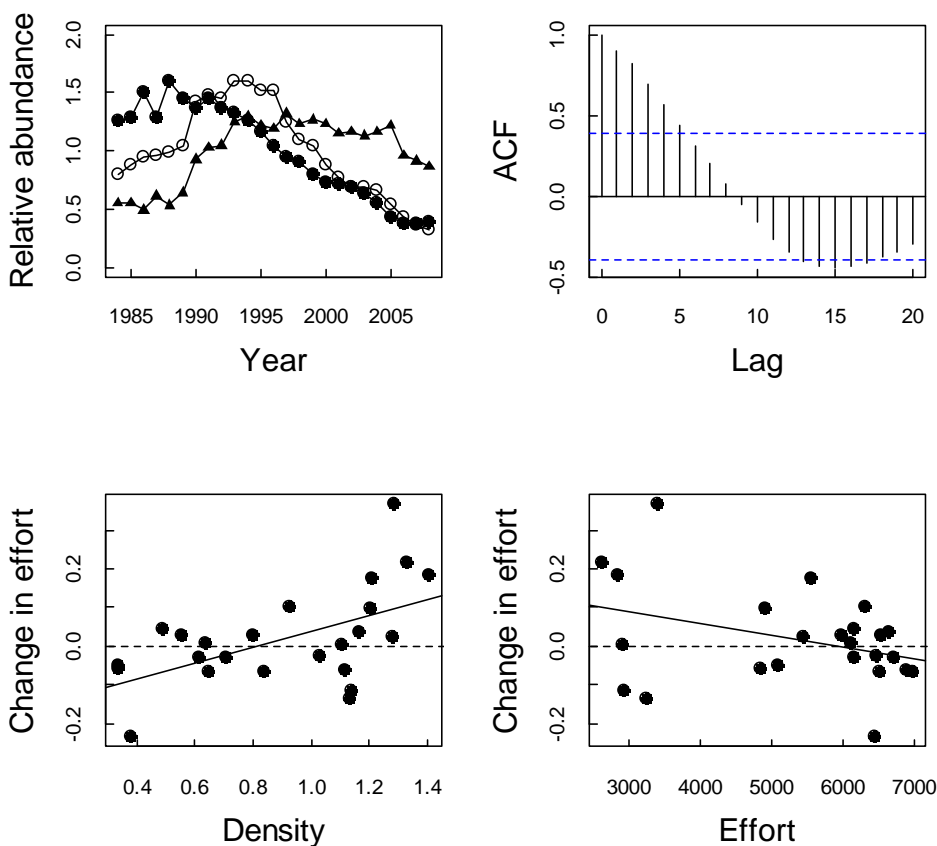


Fig. S4 – Harvest data for moose from the Troms District in Norway (resource abundance (filled circles), harvest (open circles), and effort (filled triangles)). Variables were normalized by dividing yearly values by the mean for the entire time series. Auto-correlation functions for resource abundance are shown in the right-hand plot on the top row. All correlation coefficients that exceed the horizontal bars are statistically significant (Bartlett's Test,  $P < 0.05$ ). The bottom two plots show rates of change in hunting effort ( $z$ ) in relation to resource density ( $x$ ) and current effort ( $y$ ) ( $z = 0.0112 + 0.0618x - 0.0000237y$ ,  $F_{2,16} = 6.653$ ,  $P = 0.001$ ,  $R^2 = 0.454$ ).

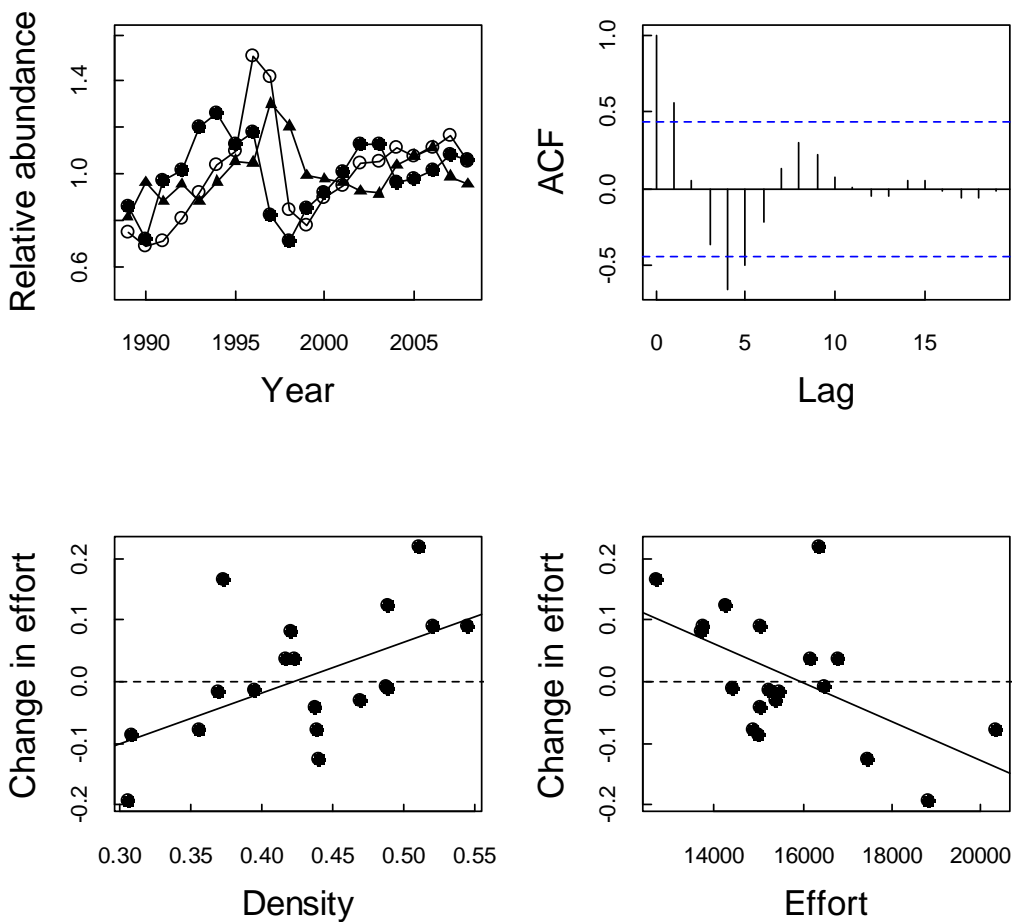


Fig. S5 – Cross-correlation functions for population density (N), harvest (H), or quota (Q) vs. effort (E) for moose in the Troms (top row), Vest Agder (middle row) Districts of Norway and white-tailed deer in the Canonto District of Ontario, Canada (bottom row). All correlation coefficients that exceed the horizontal bars are statistically significant (Bartlett's Test,  $P < 0.05$ ).

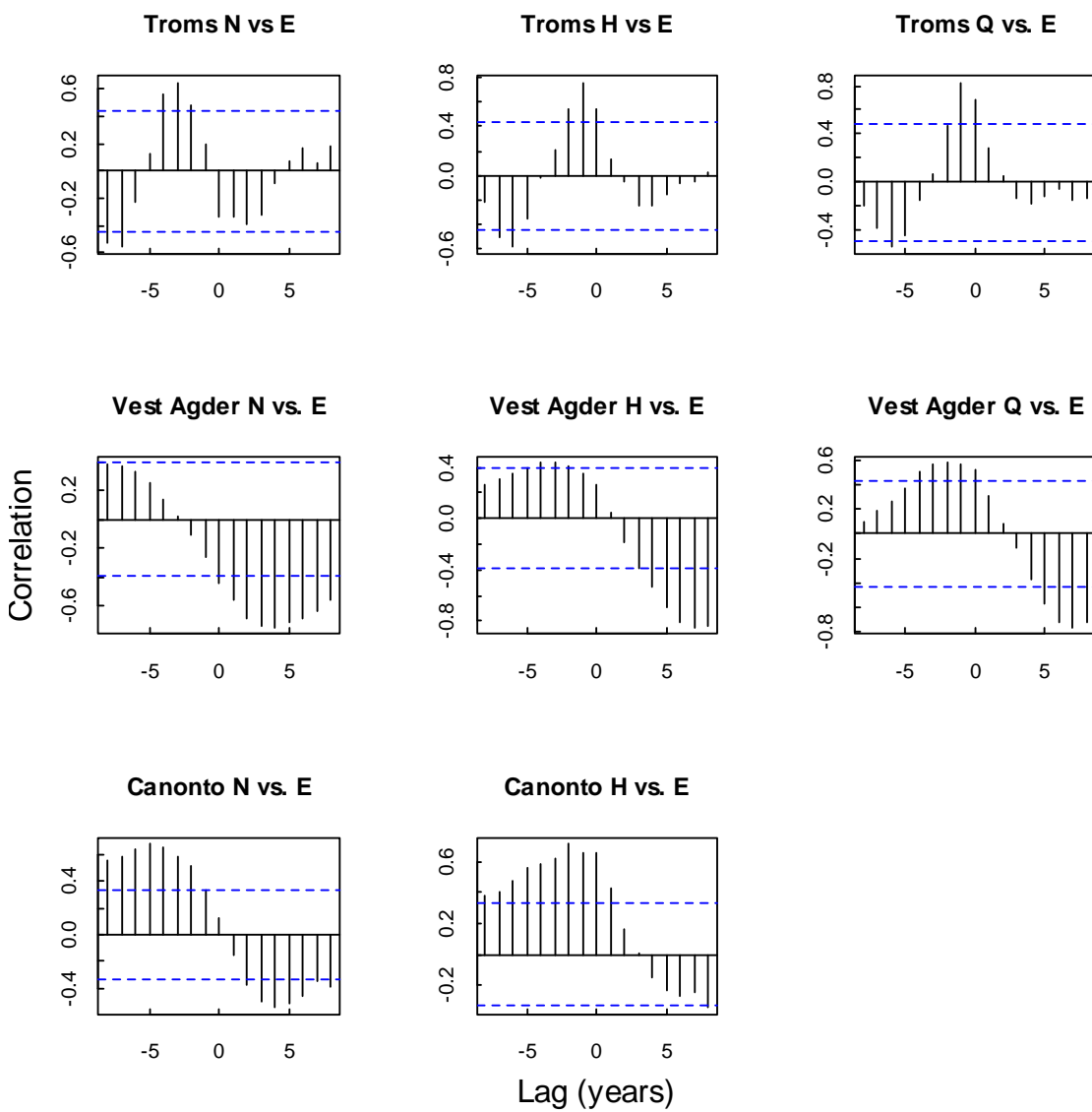


Fig. S6 – Observed rates of change in hunting quotas ( $z$ ) in relation to moose density ( $x$ ) and current quota ( $y$ ) in 2 districts of Norway (Troms:  $z = -0.143 + 1.212x - 0.000481y$ ,  $F_{2,12} = 8.381$ ,  $P = 0.005$ ,  $R^2 = 0.583$ ; Vest Agder:  $z = -0.067 + 0.250x - 0.000193y$ ,  $F_{2,17} = 6.803$ ,  $P = 0.007$ ,  $R^2 = 0.445$ ).

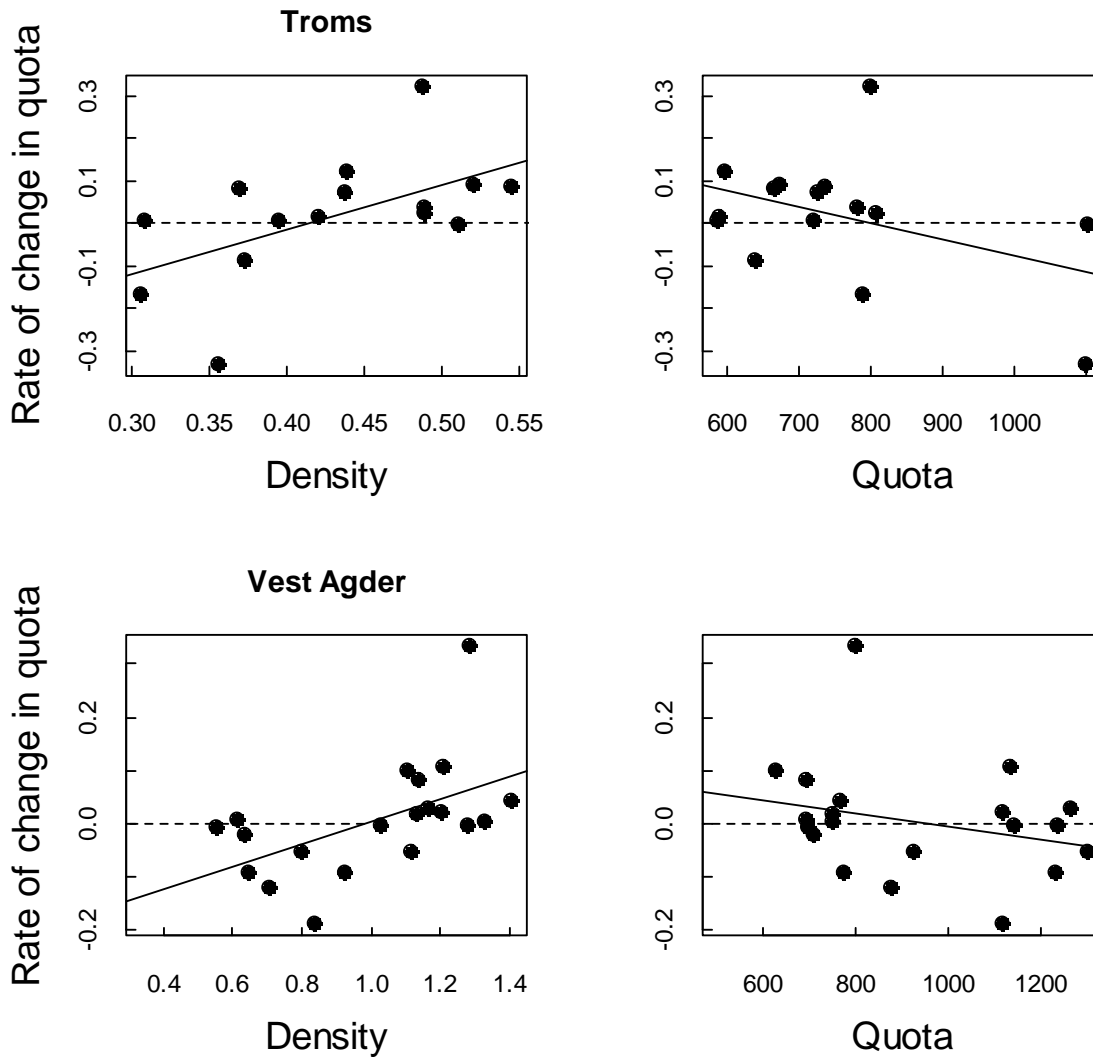


Fig. S7 – Age composition of female (top panels) and male (bottom panels) deer over time (each age class indicated by a different line type) and autocorrelation function for young of the year.

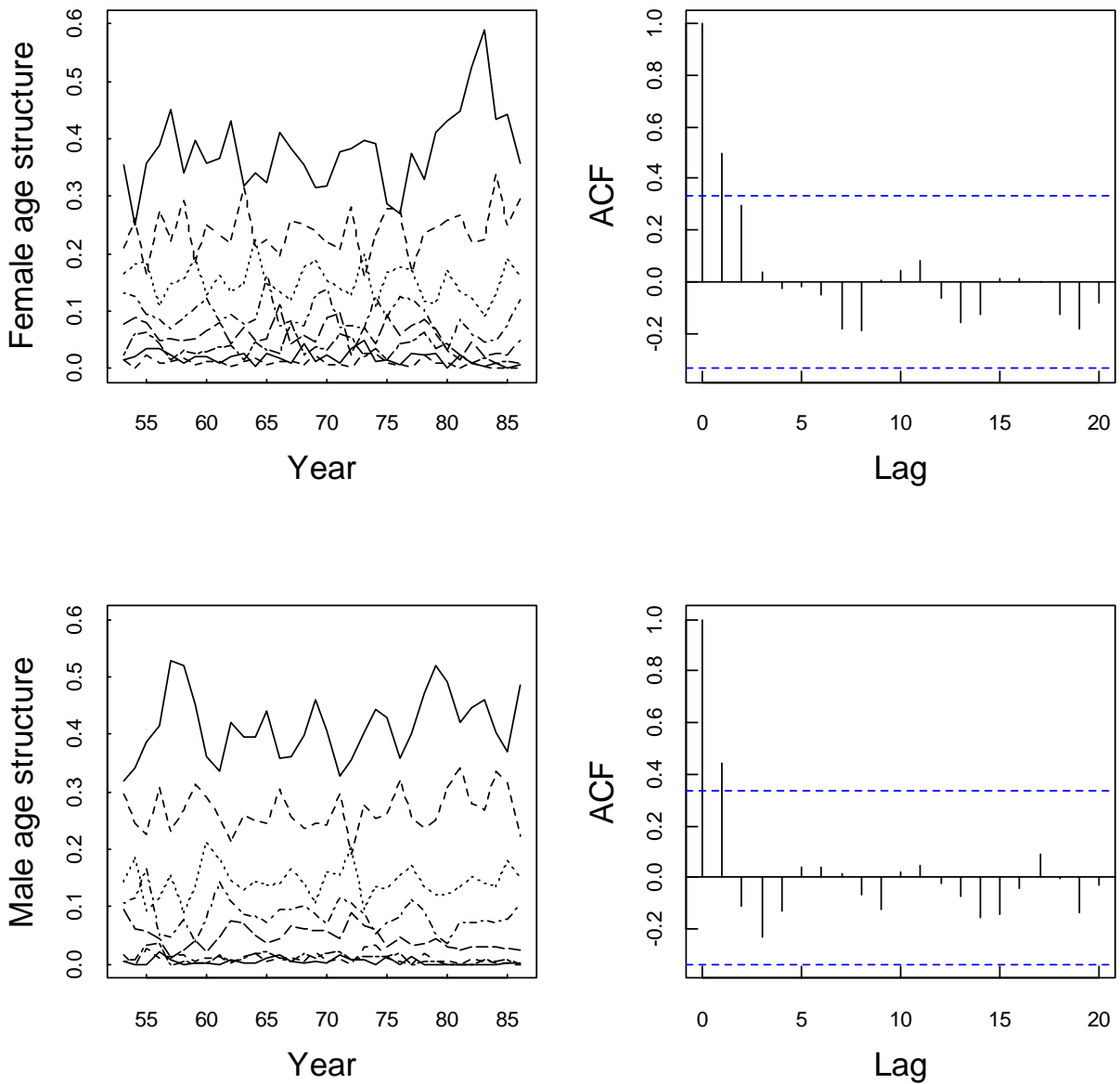
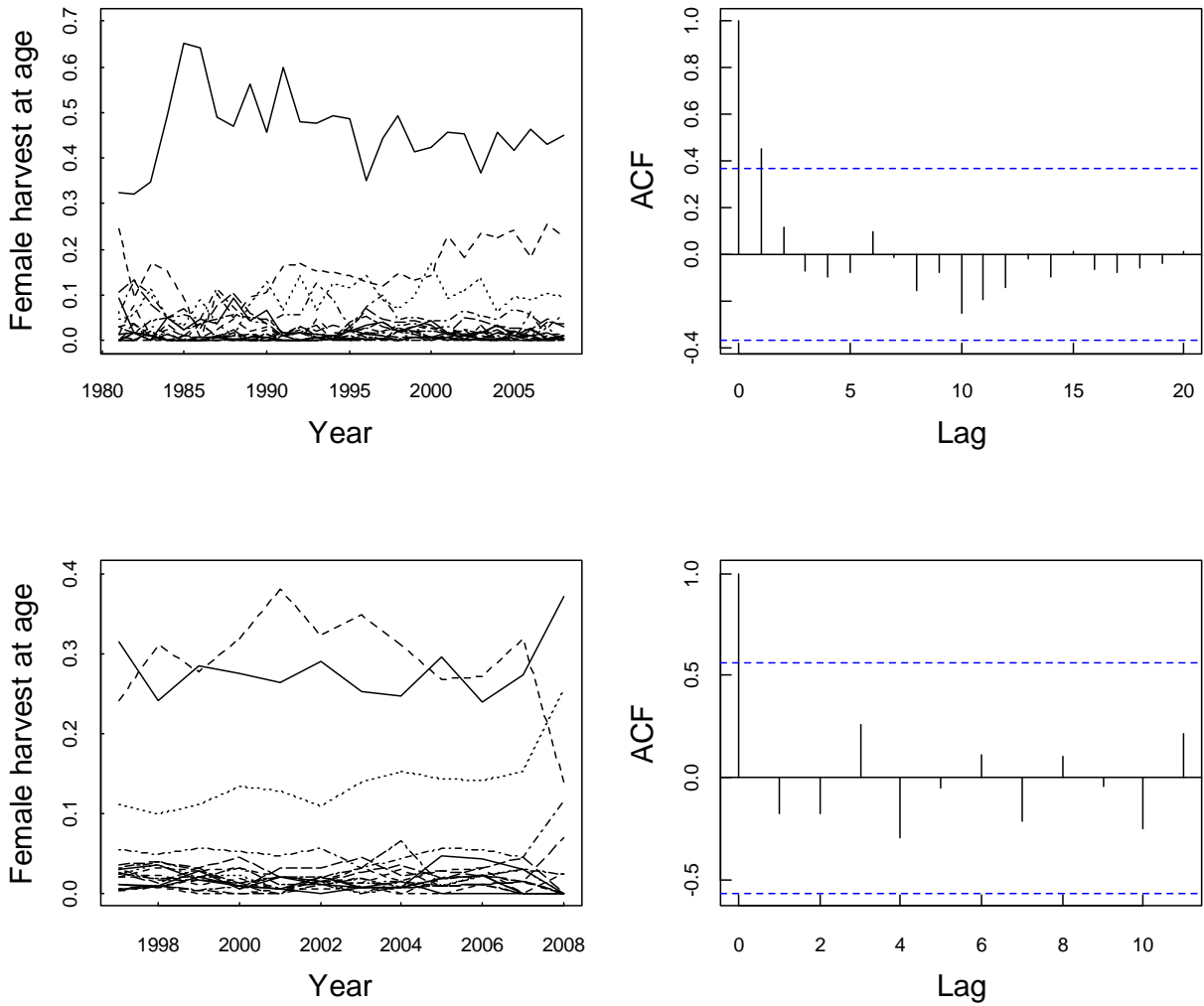


Fig. S8 – Age composition of harvest over time of female moose in Troms (top panels) and Vest Agder (bottom panels) districts in Norway (each age class indicated by a different line type) and autocorrelation function for young of the year.



## Tables

**Table 1 – Time series data for Ontario white-tailed deer.**

Year	Harvest	Effort	Deer
53	303	3830	1136
54	248	2688	839
55	154	3241	651
56	102	2299	604
57	78	2007	751
58	147	2558	951
59	134	2412	1086
60	195	2203	1176
61	196	2866	1164
62	281	2805	1298
63	195	2901	1173
64	227	3797	1189
65	262	3097	1185
66	227	2977	1109
67	238	3679	1051
68	191	3097	958
69	190	3251	951
70	226	3631	899
71	225	4171	750
72	145	3775	575
73	136	3480	516
74	107	3413	461
75	97	2938	404
76	75	2608	327
77	69	2583	302
78	75	2835	289
79	80	2889	297
80	31	1230	292
81	32	1323	364
82	28	948	516
83	72	1253	840
84	107	1554	1067
85	128	1840	1318
86	175	2303	1604

**Table 2 – Time series data for Norwegian moose**

Region	Year	Harvest	Quota	Effort	Moose
Troms	1989	453	638	12689	0.373
Troms	1990	408	585	15002	0.309
Troms	1991	425	588	13735	0.421
Troms	1992	493	596	14898	0.440
Troms	1993	550	673	13761	0.521
Troms	1994	632	735	15061	0.546
Troms	1995	669	799	16484	0.488
Troms	1996	900	1102	16349	0.512
Troms	1997	787	1098	20351	0.357
Troms	1998	507	788	18829	0.306
Troms	1999	466	665	15486	0.370
Troms	2000	541	721	15234	0.396
Troms	2001	567	726	15028	0.438
Troms	2002	629	780	14423	0.489
Troms	2003	619	807	14281	0.489
Troms	2004	688	824	16181	0.418
Troms	2005	648	NA	16813	0.424
Troms	2006	666	NA	17442	0.441
Troms	2007	675	NA	15399	0.470
Troms	2008	634	803	14920	0.458
Vest-Agder	1984	535	628	2930	1.108
Vest-Agder	1985	576	693	2944	1.137
Vest-Agder	1986	579	751	2622	1.327
Vest-Agder	1987	649	753	3260	1.133
Vest-Agder	1988	650	767	2843	1.407
Vest-Agder	1989	715	801	3412	1.283
Vest-Agder	1990	1006	1118	4926	1.206
Vest-Agder	1991	1091	1142	5441	1.280
Vest-Agder	1992	1029	1137	5568	1.211
Vest-Agder	1993	1160	1267	6645	1.166
Vest-Agder	1994	1150	1304	6885	1.114
Vest-Agder	1995	1089	1237	6475	1.031
Vest-Agder	1996	1090	1232	6310	0.923
Vest-Agder	1997	911	1121	6986	0.839
Vest-Agder	1998	803	927	6531	0.801
Vest-Agder	1999	760	877	6725	0.707
Vest-Agder	2000	630	777	6525	0.647
Vest-Agder	2001	552	709	6105	0.636
Vest-Agder	2002	520	694	6159	0.613
Vest-Agder	2003	519	698	5987	0.557
Vest-Agder	2004	434	693	6165	0.488
Vest-Agder	2005	390	NA	6445	0.378
Vest-Agder	2006	321	NA	5095	0.334
Vest-Agder	2007	269	NA	4857	0.337
Vest-Agder	2008	236	501	4582	0.340

**Table 3 – Age composition of female white-tailed deer in Canonto, Ontario**

year	age 0	age 1	age 2	age 3	age 4	age 5	age 6	age 7
53	203	120	94	75	45	14	9	9
54	107	111	78	54	38	26	9	0
55	125	57	65	33	28	22	12	8
56	127	90	36	28	16	14	11	3
57	181	89	60	28	21	6	9	5
58	155	133	72	40	22	15	4	8
59	201	94	98	53	26	14	10	3
60	199	139	71	68	36	16	11	7
61	218	138	97	50	47	23	6	7
62	299	152	93	65	30	29	14	2
63	195	193	91	48	43	10	16	8
64	210	131	138	52	30	28	3	11
65	183	126	84	91	30	18	15	3
66	222	106	73	40	60	14	10	6
67	203	138	64	44	23	42	5	6
68	174	123	87	37	28	12	21	3
69	139	105	83	57	20	17	5	11
70	138	95	67	61	39	14	10	3
71	143	78	53	27	37	23	4	3
72	117	86	39	23	7	17	11	0
73	110	44	55	19	20	6	14	7
74	99	59	27	32	11	9	3	7
75	58	56	34	18	19	3	3	2
76	43	44	28	20	9	7	1	1
77	56	25	26	18	11	7	4	0
78	42	30	15	13	11	8	3	3
79	47	28	13	7	8	4	3	1
80	40	24	16	3	3	4	0	1
81	57	34	17	11	2	3	3	0
82	114	48	27	13	10	2	2	2
83	249	95	39	19	9	7	2	2
84	258	202	77	30	15	6	5	1
85	367	208	157	61	19	11	1	1
86	362	299	161	122	49	10	8	0

**Table 4 – Age composition of harvested female moose in Troms, Norway**

Year	age											
	0	1	2	3	4	5	6	7	8	9	10	>10
1981	21	16	3	4	7	2	6	2	1	1	1	1
1982	17	5	3	7	7	1	1	2	4	0	0	6
1983	31	15	10	9	7	4	0	0	1	1	3	8
1984	39	12	4	4	4	4	4	3	2	1	1	1
1985	56	8	3	5	6	2	2	1	1	0	0	2
1986	70	1	10	5	3	4	5	1	4	4	0	2
1987	81	17	6	19	13	8	6	4	2	1	2	7
1988	82	9	2	13	18	10	16	8	3	3	2	8
1989	76	13	11	6	8	7	6	3	1	0	0	4
1990	60	14	17	5	5	6	9	4	3	1	2	5
1991	63	17	7	6	1	2	1	1	1	1	2	3
1992	60	21	18	7	4	2	2	0	3	2	4	2
1993	71	23	10	19	3	5	2	7	1	2	2	4
1994	83	25	21	15	6	1	2	3	0	2	1	9
1995	99	29	24	6	4	8	4	4	0	1	4	20
1996	117	43	47	24	23	18	11	9	6	6	9	19
1997	131	35	27	30	14	9	12	12	0	5	5	16
1998	71	21	10	7	6	3	3	3	4	0	5	11
1999	56	18	13	7	6	3	4	4	3	3	5	13
2000	65	22	26	7	5	3	7	4	1	5	4	5
2001	72	36	15	7	2	2	3	3	1	2	5	10
2002	90	36	22	13	10	5	3	5	3	2	3	6
2003	67	43	25	10	8	3	3	0	2	1	1	19
2004	77	38	11	8	5	6	6	3	1	0	2	12
2005	76	44	18	13	5	3	2	1	4	2	0	15
2006	81	32	16	10	4	2	2	2	1	2	11	12
2007	74	44	18	5	8	7	3	1	2	5	1	4
2008	75	38	16	10	5	6	1	1	3	1	0	11

**Table 5 – Age composition of harvested female moose in Vest Agder, Norway**

Year	age 0	1	2	3	4	5	6	7	8	9	10	>10
1997	108	83	38	19	12	11	10	7	7	8	10	31
1998	75	97	31	15	12	12	11	7	10	11	5	26
1999	72	70	28	14	8	7	4	3	7	5	4	31
2000	62	72	30	12	1	3	2	4	7	5	3	25
2001	50	72	24	9	6	4	1	1	4	1	4	13
2002	56	62	21	11	6	4	4	3	3	3	3	17
2003	40	55	22	5	7	5	1	5	2	0	2	14
2004	34	43	21	6	3	9	1	2	4	2	2	11
2005	31	28	15	6	3	1	5	3	1	1	1	10
2006	22	25	13	5	2	2	4	3	1	2	1	12
2007	18	21	10	3	1	2	2	0	0	2	1	6
2008	16	6	11	5	3	1	0	0	1	0	0	0

## References

- S1. J.M.C. Hutchinson, P.M. Waser. *Biol. Rev.* **82**, 335 (2007).
- S2. B.A. Melbourne, A. Hastings. *Nature* 454, 100 (2008).
- S3. M.L. Rosenzweig, R.H. MacArthur. *Am. Nat.* **97**,209 (1963).
- S4. M.L. Rosenzweig. *Science* **171**,385 (1971).
- S5. P. Yodzis. *Introduction to theoretical ecology* (Harper and Row, New York, 1989).
- S6. A. Hastings. *Population biology : concepts and models* (Springer, New York , 1997).
- S7. S.P. Otto, T. Day. *A biologist's guide to mathematical modelling* (Princeton University Press, Princeton, 2007).